Effect of minimum quantity lubrication with Al_2O_3 nanoparticles on surface roughness, tool wear and temperature dissipation in machining Inconel 600 alloy

V Vasu* and **G Pradeep Kumar Reddy**

*Department of Mechanical Engineering, NIT Warangal, Warangal, India

The manuscript was received on 24 August 2011 and was accepted after revision for publication on 3 October 2011

DOI: 10.1177/1740349911427520

Abstract: Eco-friendly machining processes are gaining importance to avoid environmental pollution. Even though cutting fluids have a reasonably low cost, their handling and carrying costs are very high and also, owing to their toxic nature, dumping of used fluids is a big problem because it can be hazardous to workers and also to the environment. To avoid these problems, a minimal-cutting-fluid technique called minimum quantity lubrication (MQL) was used in machining. Owing to the development of nanomaterials by nanotechnology techniques, the effectiveness of the cutting fluids can be increased by dispersing them. In the present work a vegetable-oil-based MQL with different volume fraction of Al_2O_3 (aluminium oxide) nanoparticles is used as the cutting fluid for machining Inconel 600 alloy. Experimental results for three different conditions – dry, MQL, MQL + Al_2O_3 nanoparticles – are plotted. It is observed that surface finish and temperature dissipation of the workpiece increase with different volume fractions of Al_2O_3 nanoparticle addition. It is also possible to observe a decrease in cutting forces and tool wear rate, and a reduction in the negative environmental effects, owing to Al_2O_3 nanoparticle addition to MQL in machining Inconel 600 alloy.

Keywords: nanofluids, MQL, Inconel 600 alloy

1 INTRODUCTION

The metal cutting process is a high energy consumption process where the energy is used to shear off the extra material and convert a raw material into a final required product that serves the necessary purposes. Owing to this high energy consumption and shearing of the material by a cutting tool, a high amount of friction will be developed and, due to this friction, an abnormal amount of temperature is generated at the tool, work, and chip interfaces, which is the main reason for the increase in cutting force, tool wear, and surface roughness [**1**]. Therefore, there is a need to control friction between the tool, work, and chip and reduce the temperature generated. For this purpose a bulk amount of cutting fluid is forced to splash on-to the cutting zone. The cutting fluid cools the cutting zone and provides lubrication for tool–chip contact, thereby reducing the friction and also the temperature generated. This provides a good surface, less tool wear, and less cutting forces during machining. Despite all of these benefits, there are also negative impacts of cutting fluids such as carrying problems, disposal problems, the toxic nature of fluid, and also the environmental pollution such as soil pollution, water pollution, and air pollution [**1**, **2**].

This need gave birth to a new technique called minimum quantity lubrication (MQL). In MQL machining, a small amount of vegetable oil is sprayed onto the cutting zone with compressed air in the form of a pulsed jet. The consumptions of vegetable oil in MQL machining will be in the range

**Corresponding author: Department of Mechanical Engineering, NIT Warangal, Warangal, India.*
email: vvvasu@gmail.com

of 10 to 100 ml/hour approximately [**2**]. Dhar *et al.* [**2**, **3**], Liao *et al.* [**4**], and Thepsonthi *et al.* [**5**] investigated MQL turning and high-speed milling of steel alloys. They found that conventional cutting fluid application fails to penetrate the chip–tool interface and thus cannot cool the heat zone effectively. Kamata and Obikawa [**6**] and Thakur *et al.* [**7**] investigated dry MQL turning of super alloys, which are widely applied in modern industry because of their superior mechanical properties such as heat and corrosion resistance, and found the MQL technique to be effective. The authors reported that in machining of super alloys, the tool wears rapidly because of a very high cutting temperature and strong adhesion between the tool and work material resulting from their low thermal conductivity and high reactivity. Therefore, particularly in this situation, the MQL technique with high thermal conductivity coolant is preferred. Owing to emerging nanotechnology, high thermal conductivity fluids called 'nanofluids' have been developed. Nanofluids are engineered colloidal suspensions of nanoparticles (10–100 nm) in base fluids [**8**]. Saidur *et al.* [**9**] presented a detailed review on applications and challenges of nanofluids. It has been found that nanofluids have a much higher and strongly temperature-dependent thermal conductivity at very low particle concentration [**10**], which is considered to be a key parameter for enhanced performance for many of the applications. Nanofluids, with their cooling and lubricating properties, have emerged as a promising solution in the application of machining. Shen *et al.* [**11**] used water-based Al_2O_3 and diamond nanofluids in the MQL grinding process. They compare the wheel wear and tribological characteristics in wet (pure water), dry, and MQL grinding processes with nanoparticle grinding of cast iron. They reported a reduction in grinding forces, improving surface roughness and lower grinding temperature with MQL nanofluids. Similarly, Malkin and Sridharan [**12**] investigated the grinding performance for MQL using ester oil with nanotubes and molybdenum disulphide nanoparticles. The authors reported better results than plain ester oil in reducing thermal distortion, owing to better lubrication and reduced specific energy. Jung *et al.* [**13**] investigated MQL with nano-diamond particles in the micro-drilling process on an aluminium 6061 workpiece. The experimental data demonstrate that the inclusion of nanoparticles in vegetable-oil-based MQL produces a significant increase in the number of drilled holes and reduction in drilling torque and thrust forces. Lee *et al.* [**14**, **15**] discuss the characteristics of nanofluid MQL meso-scale grinding and the milling process in the miniaturized machine tool system using nano-diamond particles in paraffin oil, and observed a significant reduction in cutting forces and surface roughness compared with dry and pure MQL cases.

This paper presents a study of the effect on surface roughness, tool wear, and temperature dissipation of suspending Al_2O_3 nanoparticles in eco-friendly vegetable MQL oil when machining Inconel 600 alloy at different speed-feed-depths of cut combinations by coated carbide cutting tools.

2 EXPERIMENTAL PROCEDURE

Inconel 600 alloy is a standard nickel-chromium engineering alloy which is highly corrosion resistant, and is widely used in furnace and chemical processing equipment. The workpieces have a hardness of 75HRB, with composition of 72 per cent Ni (nickel), 15 per cent Cr (chrome), 7 per cent Fe (iron), 1 per cent Mn (manganese), 0.5 per cent Si (silicon), and 0.15 per cent C (carbon). Multicoated inserts CNMG 1 20 408 with P30 ISO specification from KORLOY, Korea, with a tool holder of PCLNR 1616H12, are used in the present study. Figure 1 shows the experimental set-up for the present studies: an Inconel 600 alloy rod of initial diameter 20 mm and length 100 mm is machined using coated carbide cutting tools by a precision engine lathe machine. Different speed-feed-depth of cut combinations (see Table 1) under dry condition, MQL condition, MQL with 4 per cent volume fraction of Al_2O_3 nanofluid, and MQL with 6 per cent volume fraction of Al_2O_3 nanofluid condition are used in the study. The machinability characteristics of the work material at different conditions are considered, mainly regarding surface roughness, tool wear, cutting forces, and temperature dissipation. The MQL needs to be supplied at high pressure and impinged at high speed through the nozzle at the cutting zone. Considering the conditions of the present study, an uninterrupted supply of MQL at constant pressure around 5 bar is required.

2.1 Selection of the factors and their levels under Taguchi's approach

A total of 36 experiments based on Taguchi's L9 orthogonal array [**16**] were carried out with different combinations of the levels of the input parameters as shown in Table 2. In the Taguchi method, the term 'signal' represents the desirable value (mean) for the output characteristic and the term 'noise' represents the undesirable value (SD) for the output

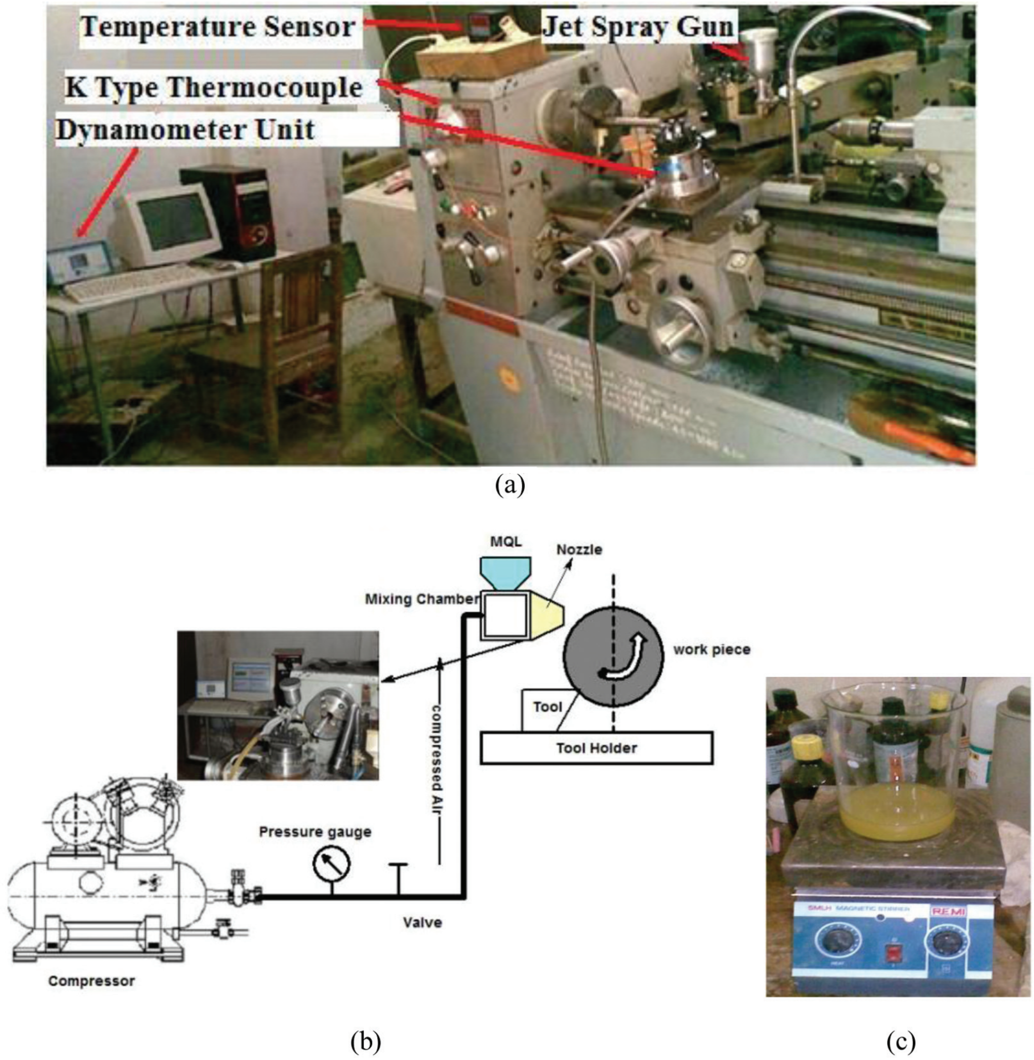

Fig. 1 (a) Photographic view of the experimental set-up; (b) schematic view of MQL system; (c) mixing of MQL and Al_2O_3 nanoparticles using magnetic stirrer

Table 1 Experimental specifications

Machine tool	Precision engine lathe, capacity 4.5 V
Workpiece	Inconel 600 (dia. 20 mm)
Cutting tool	Coated carbide inserts
Insert code system	CNMG1 20 408−HF
Cutting velocity, V_c	40, 50, and 60 m/min
Feed rate, f	0.08, 0.12, and 0.16 mm/rev
Depth of cut, t	0.4, 0.8, and 1.2 mm
MQL supply	Air: 5 bar, lubricant: 100 ml/h
Vegetable oil	Coolube 2210^{EP}
Nanoparticles	Al_2O_3
Environment	Dry, minimum quantity lubrication (MQL) and MQL with nanofluids (4% volume fraction of Al_2O_3 and 6% volume fraction of Al_2O_3).

Table 2 Process parameters and their levels

Factor	Unit	Level 1	Level 2	Level 3
Cutting speed	m/min	40	50	60
Feed	mm/rev	0.08	0.12	0.16
Depth of cut	mm	0.4	0.8	1.2

characteristic. Therefore, the S/N ratio represents the amount of variation present in the quality characteristic. The S/N ratio is the ratio of the mean to the SD. Taguchi uses the S/N ratio to measure the quality characteristic deviating from the desired value. The S/N ratio η is defined as

$$\eta = -10\log(\mathrm{MSD}) \quad (1)$$

where MSD is the mean-square deviation for the output characteristic.

Here the desirable objectives are lower values of surface roughness and tool wear. Therefore, the lower-the-better type S/N ratio, as given below, was applied for transforming the observed data

$$\eta = -10 \log \left(\frac{1}{n} \sum_{i=1}^{n} y_i^2 \right) \tag{2}$$

where η is the S/N ratio for the lower-the-better case, y_i the measured quality characteristic for the ith repetition, n the number of repetitions in a trial.

Tables 3–6 (in the Appendix) show the experimental results for surface roughness, tool tip temperature, cutting force and tool life, and the corresponding S/N ratio for both under different environment conditions using equation (2). From experimental results, the optimal level of cutting parameter affecting the quality characteristic continuously under different environment conditions, i.e. dry, MQL, MQL with 4% vol. Al_2O_3 nanoparticles, and MQL with 6% vol. Al_2O_3 nanoparticles, are obtained (see the Appendix).

Once the optimal level of the design parameters has been selected, the final step is to predict and verify the improvement of the quality characteristic using the optimal level of the design parameters (Tables 7(a) to 7(d) in the Appendix). The estimated S/N $\hat{\eta}$ ratio using the optimal level of the design parameters can be calculated as [**17**]

$$\hat{\eta} = \eta_m + \sum_{i=1}^{k} (\bar{\eta}_i - \eta_m)$$

where η_{m} is the total mean S/N ratio, $\bar{\eta}_i$ is the mean S/N ratio at the optimal level, and k is the number of the main design parameters that affect the quality characteristic.

3 RESULTS AND DISCUSSION

From the Fig. 2 Taguchi optimization results, it is found that MQL + Al_2O_3 nanoparticles show reduction in surface roughness, tool tip temperature, cutting forces, and tool wear than dry and plain MQL conditions, and it also gives better chip formation than both cutting conditions.

3.1 Surface roughness

Surface roughness plays an important role on the performance of a product and product failure before the expected life owing to appalling surface. In the present work, surface roughness of the workpiece was measured by a Taylor-Hobson Surtronic 3+ Talysurf with a resolution of 0.01 μm, traverse length of 0.25 mm, and traverse speed of 1 mm/s. In general, low surface finish is possible with high cutting speed and low feed rate without considering any wear during machining. Figure 2(a) indicates that there is a reduction of surface roughness in the MQL + 6% Al_2O_3 nanofluid condition as compared to dry, and MQL, MQL + 4% Al_2O_3 nanofluids. This could be attributed to more intensive temperature and stresses at tool–chip interface in the dry cutting condition. It is observed that plain MQL condition give a better surface finish than the dry cutting process, depending on controlling the deterioration of the auxiliary cutting edge of abrasion, chipping, and built-up edge formation. It is also observed that MQL + 6% Al_2O_3 nanofluid further decreases in surface roughness; this is because nanofluids exhibit enhanced thermal properties such as higher thermal conductivity and heat transfer coefficients compared with the plain MQL.

3.2 Tool tip interface temperature

During machining, heat is generated [**1**] at the (a) primary deformation zone due to shear and plastic deformation, (b) chip–tool interface owing to secondary deformation and sliding, and (c) work–tool interfaces due to rubbing. All such heat sources have a significant influence on the cutting forces, tool life, and chip formation mode. Conventional cutting fluids cannot cool and lubricate effectively as expected and become more ineffective as the cutting speeds increase, owing to reduction in chip tool contact length. A standard K-type thermocouple mounted at the site of the tool–work junction directly monitored the tool tip interface temperature using a digital temperature indicator. Figure 2(b) indicates that there is a reduction of tool tip interface temperatures in MQL + 6% Al_2O_3 nanofluid condition as compared to dry, MQL, and MQL + 4% Al_2O_3 nanofluids. As in MQL machining, cooling occurs by convective and evaporative heat transfer of coolant.

As MQL + 6% Al_2O_3 nanofluid will have a higher thermal conductivity, it will have a higher convective heat transfer coefficient [**10**]. It was observed that MQL + 6% Al_2O_3 nanofluid enabled a reduction of the average tool tip interface temperature by about 12 to 20 per cent, depending upon the levels of the process parameters, which will have a favourable influence on the machinability of the workpiece.

3.3 Cutting forces

Cutting force is the vital parameter to be considered in the design of the machine–fixture-tool-work systems. In the present work the cutting forces are calculated by using a four-component piezo electric Kistler dynamometer. It is evident from

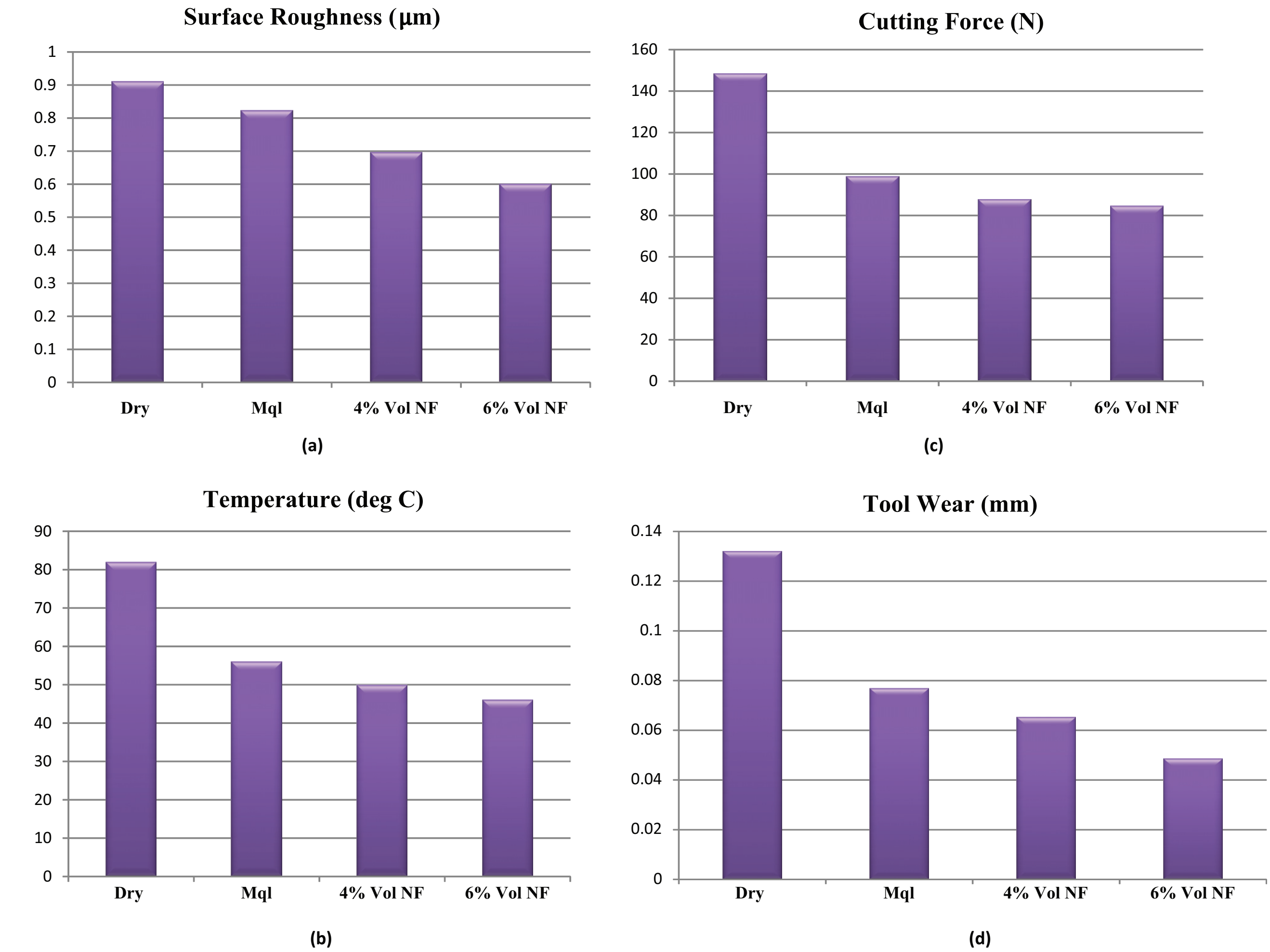

Fig. 2 Response graphs at optimal cutting parameters

Fig. 2(c) that there is a reduction of cutting forces in MQL + 6% Al_2O_3 nanofluid condition as compared to dry, MQL, and MQL + 4% Al_2O_3 nanofluids at all the experimental combinations. This can be attributed to reduction of cutting zone temperatures, which results in less friction and a decrease in the formation of built-up edges. It was observed that MQL + 6% Al_2O_3 nanofluid enabled a reduction of 30 to 35 per cent of cutting forces.

3.4 Tool wear

The flank wear was caused by continuous rubbing of the work material with cutting edges. The extent to which the wear occurs depends upon many factors such as work material hardness, operating parameters, properties of cutting edges and coolant, and low thermal conductivity of materials, etc. Inconel 600 low thermal conductivity material is difficult to machine due to less softening of the material. Therefore, the supply of coolant plays an important role in tool wear. The average width of the principal flank wear was measured using a metallurgical microscope (Carl Zesis, 3 51 396, Germany) fitted with a micrometer of least count 1 µm. Figure 2(d) and Figure 3 indicate a reduction of tool wear in MQL + 6% Al_2O_3 nanofluid condition as compared to dry, MQL, and MQL + 4% Al_2O_3 nanofluids. The tool life was increased by 45 per cent by MQL + 6% Al_2O_3 nanofluids as coolant than dry cutting. This is because at high cutting speed, the coolant may not have enough time to remove heat accumulated at the cutting zone, resulting in less reduction of temperature under plain MQL and dry cutting, which leads to more predominant built-up edge formation and an increase in tool wear. However, in MQL + Al_2O_3 nanofluid machining conditions, nanofluids help to reduce the temperature, resulting in a decrease of built-up edge formation because of the enhanced thermophysical properties of nanofluids.

3.5 Chip formation

Figure 4 indicates spiral type chips; the colour of the chips is brown in dry condition. In MQL the form of

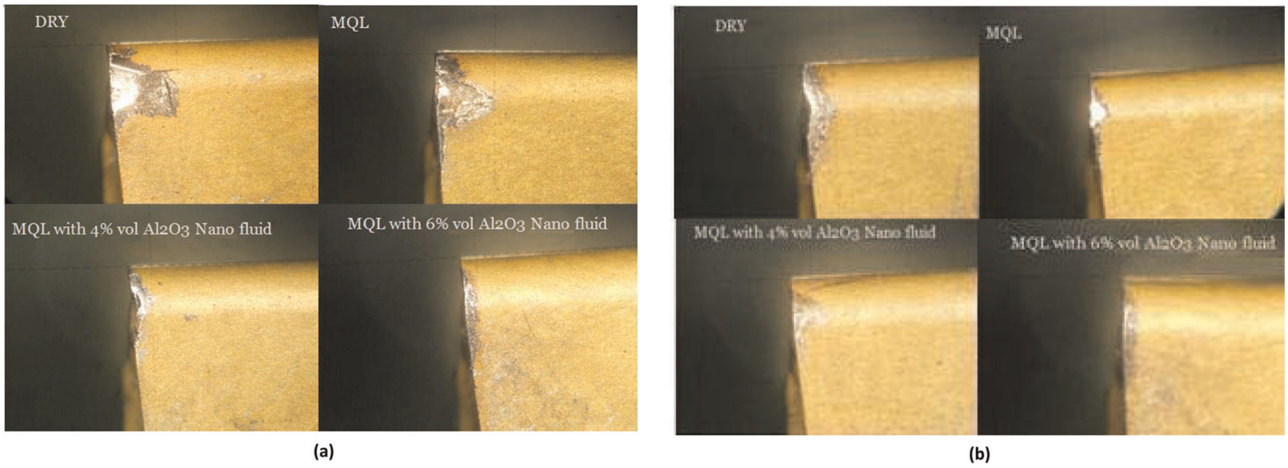

Fig. 3 Tool wear at respective cutting parameters: (a) speed = 40 m/min, feed = 0.16 mm/rev, depth = 1.2 mm; (b) speed = 60 m/min, feed = 0.16 mm/rev, depth = 0.4 mm

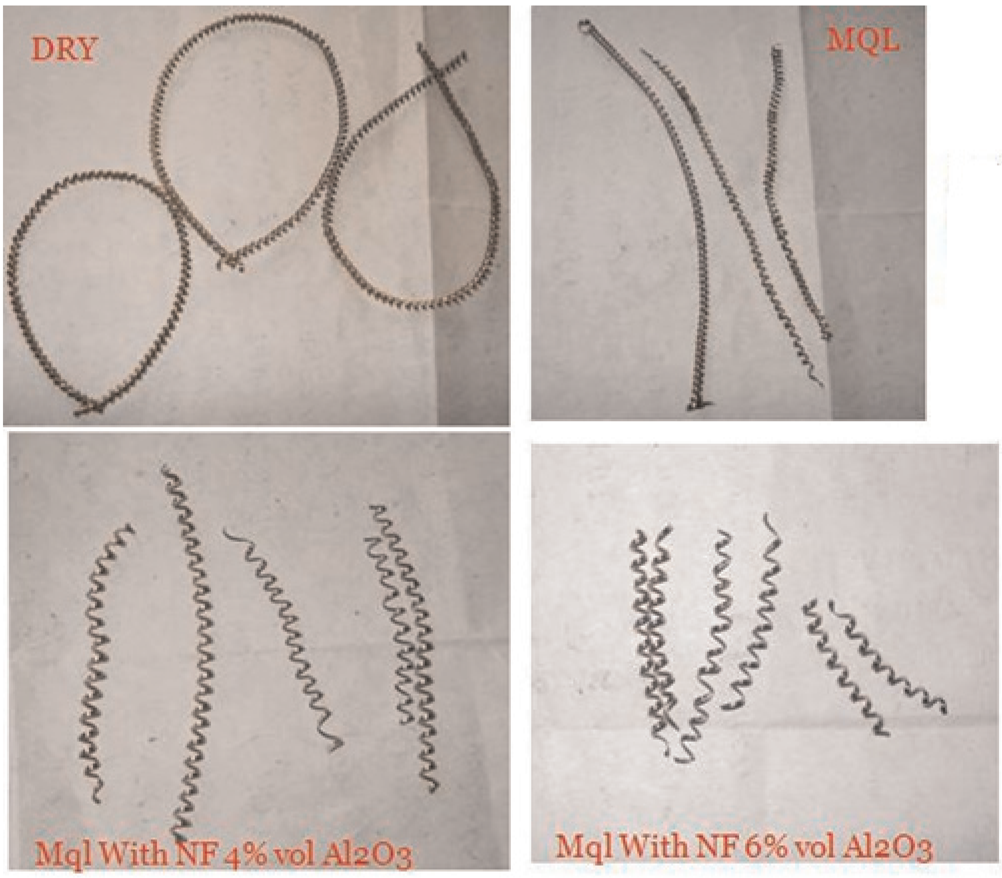

Fig. 4 Chips obtained in machining Inconel 600 at different environments at speed = 40 m/min, feed = 0.16 mm/rev, DOC = 1.2

the chips changes appreciably into more or less half turn and their back surface appears slightly lighter and smoother. However, chips in MQL with Al_2O_3 nanofluid chips do not change appreciably than plain MQL condition, but the continuity is decreased and the colour of the chips becomes much lighter, i.e. metallic from brown. This shows that the temperature and cutting forces are reduced while machining with MQL with different volume concentrations of Al_2O_3 nanoparticles.

4 CONCLUSIONS

The following conclusions can be drawn based on the experimental results.

1. The performance of the MQL technique with Al_2O_3 nanoparticle nanofluids could reduce many cutting problems caused by the high consumption of lubricant, such as high machining cost, and environmental and worker-health problems.
2. The experimental results demonstrate that the feed rate is the main parameter among the three controllable factors (cutting speed, feed rate, and depth of cut) that influence the surface roughness in machining Inconel 600 alloy.
3. The experimental results demonstrate that the depth of cut is the main parameter among the three controllable factors (cutting speed, feed rate, and depth of cut) that influence the temperature generated while machining Inconel 600 alloy.
4. The experimental results demonstrate that the feed rate and depth of cut are the main parameters among the three controllable factors (cutting speed, feed rate, and depth of cut) that influence the cutting force in machining Inconel 600 Alloy.
5. The experimental results demonstrate that the feed rate and depth of cut are the main parameters among the three controllable factors (cutting speed, feed rate, and depth of cut) that influence the tool wear in machining Inconel 600 alloy.
6. The experimental results show that surface roughness, temperature, cutting force, and tool wear can be reduced significantly by machining Inconel 600 alloy under the condition of MQL with (6 vol.% of Al_2O_3 particle) nanofluids than dry and MQL.

FUNDING

This research received no specific grant from any funding agency in the public, commercial, or not-for-profit sectors.

REFERENCES

1 **Byers, J. P.** *Metal working fluids*, first edition, 1994 (CRC, USA).

2 **Rahman, M. M., Khan, M. M. A.,** and **Dhar, N. R.** An experimental investigation into the effect of minimum quality lubricant on cutting temperature for machinability of AISI 9310 steel alloy. *Eur. J. Sci. Res.*, 2009, **29**(4), 502–508.

3 **Dhar, N. R., Islam, S., Islam, M. W.,** and **Mithu, M. A. H.** The influence of minimum quantity of lubrication (MQL) on cutting temperature, chip and dimensional accuracy in turning AISI-1040 steel. *J. Mater. Processing Technol.*, 2006, **171**, 93–99.

4 **Liao, Y. S., Lin, H. M.,** and **Chen, Y.** Feasibility study of the minimum quantity lubrication (MQL) in high-speed end milling of NAK80 hardened steel by coated carbide tool. *Int. J. Machine Tools Mf.*, 2007, **47**, 1667–1676.

5 **Thepsonthi, T., Hamdi, M.,** and **Mitsui, K.** Investigation into minimal-cutting-fluid application in high-speed milling of hardened steel using carbide mills. *Int. J. Machine Tools Mf.*, 2009, **49**, 156–162.

6 **Kamata, Y.** and **Obikawa, T.** High speed MQL finish turning of Inconel 718 with coated tools. *J. Mater. Processing Technol.*, 2007, **192**, 251–256.

7 **Thakur, D. G., Ramamoorthy, B.,** and **Vijayaraghavan, L.** Optimization of minimum quantity lubrication parameters in high speed turning of superalloy Inconel 718 for sustainable development. *World Acad. Sci., Engng Technol.*, 2009, **54**, 224–226.

8 **Eastman, J. A., Phillpot, S. R., Choi, S. U. S.,** and **Keblinski, P.** Thermal transport in nanofluids. *A. Rev. Mater. Res.*, 2004, **34**, 219–230.

9 **Saidur, R., Leong, K. Y.,** and **Mohammad, H. A.** A review on applications and challenges of nanofluids. *Renewable and Sustainable Energy Rev.*, 2011, **15**(3), 1646–1668.

10 **Vasu, V., Rama Krishna, K.,** and **Kumar, A. C. S.** Exploitation of thermal properties of fluids embedded with nanostructured materials. *Int. Energy J.*, 2007. **8**(3), 178–186.

11 **Shen, B., Shih, A. J., Tung, S. C.,** and **Hunter, M.** Application of nanofluids in minimum quantity lubrication grinding. *Tribology Trans.*, 2008, **51**(6), 730–737.

12 **Malkin, S.** and **Sridharan, U.** Effect of minimum quantity lubrication (MQL) with nanofluids on grinding behavior and thermal distortion. *Trans. NAMRI/SME*, 2009, **37**, 629–636.

13 **Jung, S., N., Lee, P.-H.,** and **Lee, S. W.** Experimental characterization of micro-drilling process using nanofluid minimum quantity lubrication. *Int. J. Machine Tools Mf.*, 2011, **51**(7-8), 649–652.

14 **Lee, P.-H., Nam, T-S., Li, C.,** and **Lee, S. W.** Experimental study on meso-scale milling process using nanofluid minimum quantity lubrication and compressed chilly air. In Proceedings of the International Conference on *Mechanical, industrial, and manufacturing technologies* (MIMT 2010), Sanya, China, 2010, pp. 457–463.

15 **Lee, P.-H., Nam, T.-S., Li, C.,** and **Lee, S. W.** Environmentally-friendly nano-fluid minimum quantity lubrication (MQL) meso-scale grinding process using nano-diamond particles. In Proceedings of the International Conference on *Manufacturing automation* (ICMA), the Chinese University of Hong Kong, Hong Kong, 2010, pp. 44–49.

16 **Phillip, J. R.** *Taguchi techniques for quality engineering*, 2000 (Tata McGraw-Hill, USA).

17 **Yang, W. H.** and **Tarng, Y. S.** Design optimization of cutting parameters for turning operations based on the Taguchi method. *J. Mater. Processing Technol.* 1998, **84**, 122–129.

APPENDIX

Table 3 S/N ratios table (dry condition)

Run	Cutting speed V_c (m/min)	Feed f (mm/rev)	DOC d (mm)	S/N ratio for Ra	S/N ratio for temperature	S/N ratio for force	S/N ratio for wear
1	40	0.08	0.4	−2.8603	−38.276	−45.621	15.4423
2	40	0.12	0.8	−6.7172	−42.607	−49.158	13.4324
3	40	0.16	1.2	−9.0357	−45.845	−50.906	0.273 52
4	50	0.08	1.2	−0.612	−44.811	−47.872	1.927 35
5	50	0.12	0.4	−3.2274	−40.506	−45.105	16.9542
6	50	0.16	0.8	−5.1392	−44.959	−48.881	1.514 41
7	60	0.08	0.8	0.175 48	−42.798	−47.64	8.873 95
8	60	0.12	1.2	−4.1742	−45.437	−50.931	1.555 87
9	60	0.16	0.4	−3.3286	−44.028	−45.854	6.178 37
			Mean	−3.8799	−43.252	−47.996	7.350 27

Table 3(a) S/N response table for surface roughness (dry condition)

	Cutting parameter	Mean S/N ratio (dB)				Main effects plot
		Level 1	Level 2	Level 3	Max−Min	
A	Cutting speed	−6.2044	−2.9928	−2.4424	3.761 96	
B	Feed rate	−1.0989	−4.7062	−5.8345	4.735 56	
C	Depth of cut	−3.1388	−3.8936	−4.6073	1.468 56	

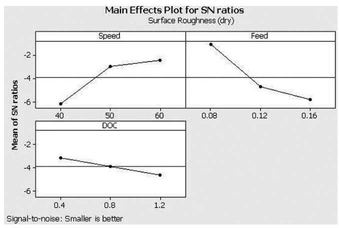

Table 3(b) S/N response table for temperature (dry condition)

	Cutting parameter	Mean S/N ratio (dB)				Main effects plot
		Level 1	Level 2	Level 3	Max−Min	
A	Cutting speed	−42.243	−43.426	−44.087	1.844 76	
B	Feed rate	−41.962	−42.85	−44.944	2.982 56	
C	Depth of cut	−40.937	−43.455	−45.364	4.427 53	

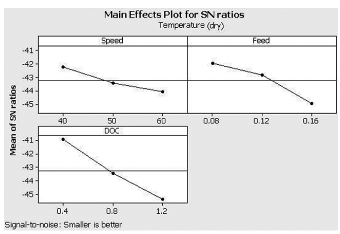

Table 3(c) S/N response table for cutting force (dry condition)

	Cutting parameter	Mean S/N ratio (dB)				Main effects plot
		Level 1	Level 2	Level 3	Max−Min	
A	Cutting speed	−48.561	−47.286	−48.142	1.275 53	
B	Feed rate	−47.044	−48.398	−48.547	1.502 84	
C	Depth of cut	−45.527	−48.56	−49.903	4.376 13	

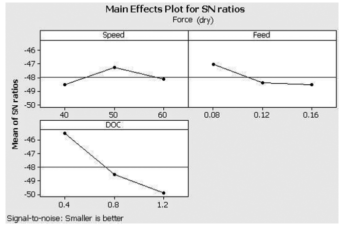

Table 3(d) S/N response table for tool wear (dry condition)

	Cutting parameter	Mean S/N ratio (dB)				Main effects plot
		Level 1	Level 2	Level 3	Max−Min	
A	Cutting speed	9.716	6.798 67	5.536 06	4.18	
B	Feed rate	8.747	10.6475	2.655 44	7.992 07	
C	Depth of cut	12.85	7.940 26	1.252 25	11.606	

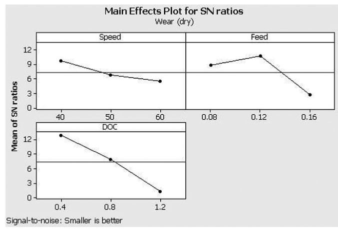

Table 4 S/N ratios table (MQL condition)

Run	Cutting speed V_c (m/min)	Feed f (mm/rev)	DOC d (mm)	S/N ratio for Ra	S/N ratio for temperature	S/N ratio for force	S/N ratio for wear
1	40	0.08	0.4	1.692	−34.964	−41.72	19.3315
2	40	0.12	0.8	−1.7698	−40.172	−47.872	16.1934
3	40	0.16	1.2	−3.2871	−44.402	−49.335	0.771 58
4	50	0.08	1.2	0.291 47	−43.405	−44.846	2.102 61
5	50	0.12	0.4	−2.232	−38.17	−42.842	20.0873
6	50	0.16	0.8	−4.2438	−43.637	−47.517	2.270 19
7	60	0.08	0.8	1.483 45	−41.138	−46.618	9.682 52
8	60	0.12	1.2	−4.1903	−44.297	−50.076	1.808 88
9	60	0.16	0.4	−2.9226	−42.345	−45.105	8.404 33
			Mean	−1.6865	−41.392	−46.214	8.961 37

Table 4(a) S/N response table for surface roughness (MQL condition)

	Cutting parameter	Mean S/N ratio (dB)				Main effects plot
		Level 1	Level 2	Level 3	Max−Min	
A	Cutting speed	−1.1216	−2.0614	−1.8765	0.9398	
B	Feed rate	1.1556	−2.7307	−3.4845	4.6401	
C	Depth of cut	−1.1542	−1.51	−2.3953	1.241 12	

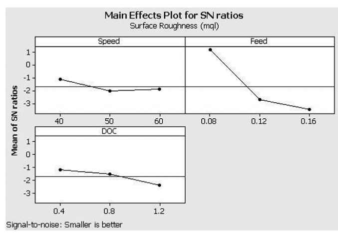

Table 4(b) S/N response table for temperature (MQL condition)

	Cutting parameter	Mean S/N ratio (dB)				Main effects plot
		Level 1	Level 2	Level 3	Max−Min	
A	Cutting speed	−39.846	−41.737	−42.593	2.747 49	
B	Feed rate	−39.836	−40.88	−43.461	3.625 79	
C	Depth of cut	−38.493	−41.649	−44.035	5.5418	

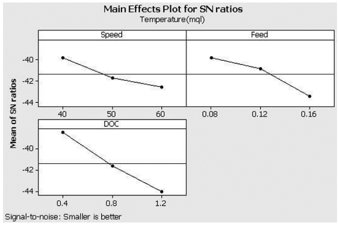

Table 4(c) S/N response table for cutting force (MQL condition)

	Cutting parameter	Mean S/N ratio (dB)				Main effects plot
		Level 1	Level 2	Level 3	Max−Min	
A	Cutting speed	−46.309	−45.068	−47.266	2.198 18	
B	Feed rate	−44.395	−46.93	−47.319	2.924 61	
C	Depth of cut	−43.222	−47.335	−48.086	4.8632	

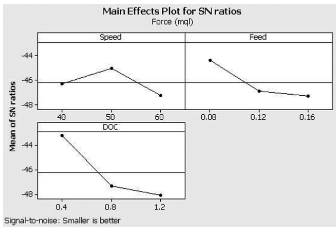

Table 4(d) S/N response table for tool wear (MQL condition)

	Cutting parameter	Mean S/N ratio (dB)				Main effects plot
		Level 1	Level 2	Level 3	Max−Min	
A	Cutting speed	12.098	8.153 36	6.631 91	5.466 91	
B	Feed rate	10.372	12.6965	3.815 36	8.881 15	
C	Depth of cut	15.941	9.382 02	1.561 02	14.38	

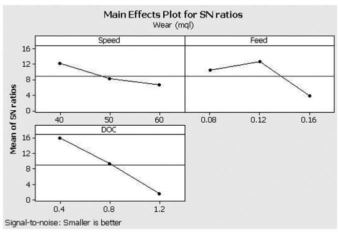

Table 5 S/N ratios table (MQL with 4% vol. Al_2O_3 nanoparticles condition)

Run	Cutting speed V_c(m/min)	Feed f (mm/rev)	DOC d (mm)	S/N ratio for Ra	S/N ratio for temperature	S/N ratio for force	S/N ratio for wear
1	40	0.08	0.4	3.147 82	−33.979	−39.007	21.2096
2	40	0.12	0.8	−0.9299	−38.79	−47.694	18.3443
3	40	0.16	1.2	−1.5836	−43.807	−48.799	1.545 49
4	50	0.08	1.2	1.8303	−43.167	−43.522	2.349 51
5	50	0.12	0.4	−1.5328	−37.73	−44.67	20.1755
6	50	0.16	0.8	−4.1635	−43.346	−46.878	3.4785
7	60	0.08	0.8	1.692	−41.062	−46.277	9.682 52
8	60	0.12	1.2	−3.9731	−44.137	−49.655	1.959 94
9	60	0.16	0.4	−2.7976	−42.007	−44.959	9.4991
			Mean	−0.9234	−40.892	−45.718	9.804 94

Table 5(a) S/N response table for surface roughness (nanofluid with 4% vol. Al_2O_3 nanoparticles)

	Cutting parameter	Mean S/N ratio (dB)				Main effects plot
		Level 1	Level 2	Level 3	Max−Min	
A	Cutting speed	0.2114	−1.2887	−1.6929	1.904 34	
B	Feed rate	2.2233	−2.1453	−2.8482	5.071 59	
C	Depth of cut	−0.3942	−1.1338	−1.2422	0.847 96	

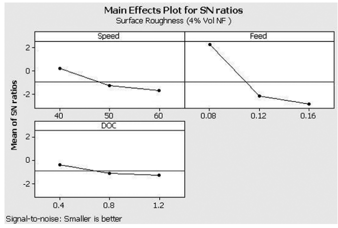

Table 5(b) S/N response table for temperature (nanofluid with 4% vol. Al_2O_3 nanoparticles)

	Cutting parameter	Mean S/N ratio (dB)				Main effects plot
		Level 1	Level 2	Level 3	Max−Min	
A	Cutting speed	−38.859	−41.414	−42.402	3.543 03	
B	Feed rate	−39.403	−40.219	−43.053	3.650 72	
C	Depth of cut	−37.906	−41.066	−43.703	5.797 93	

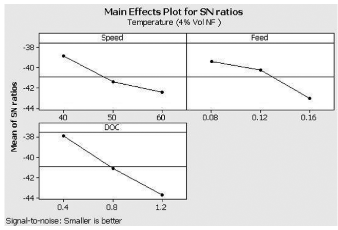

Table 5(c) S/N response table for cutting force (nanofluid with 4% vol. Al_2O_3 nanoparticles)

	Cutting parameter	Mean S/N ratio (dB)				Main effects plot
		Level 1	Level 2	Level 3	Max−Min	
A	Cutting speed	−45.167	−45.023	−46.964	1.940 54	
B	Feed rate	−42.935	−47.339	−46.879	4.403 98	
C	Depth of cut	−42.879	−46.95	−47.325	4.446 46	

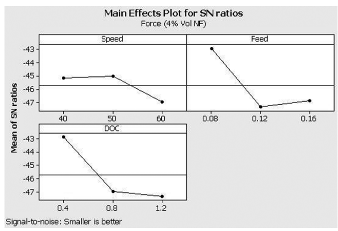

Table 5(d) S/N response table for tool wear (nanofluid with 4% vol. Al_2O_3 nanoparticles)

	Cutting parameter	Mean S/N ratio (dB)				Main effects plot
		Level 1	Level 2	Level 3	Max−Min	
A	Cutting speed	13.699	8.667 83	7.047 19	6.652 61	
B	Feed rate	11.080	13.4932	4.841 03	8.6522	
C	Depth of cut	16.961	10.5018	1.951 65	15.0098	

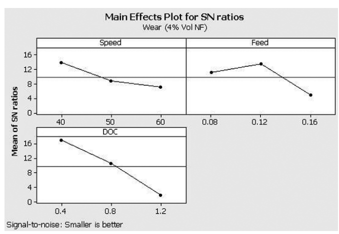

Table 6 S/N ratios table (nanofluid with 6% vol. Al_2O_3 nanoparticles condition)

Run	Cutting speed V_c (m/min)	Feed f (mm/rev)	DOC d (mm)	S/N ratio for Ra	S/N ratio for temperature	S/N ratio for force	S/N ratio for wear
1	40	0.08	0.4	4.436 97	−33.255	−38.853	22.3837
2	40	0.12	0.8	−0.1975	−38.17	−47.64	20.1755
3	40	0.16	1.2	−1.1381	−43.464	−48.742	1.808 88
4	50	0.08	1.2	2.047 46	−43.046	−43.368	2.395 16
5	50	0.12	0.4	0.509 77	−37.266	−44.185	23.7417
6	50	0.16	0.8	−3.8234	−43.227	−46.618	3.917 21
7	60	0.08	0.8	1.618 44	−40.906	−46.277	9.842 88
8	60	0.12	1.2	−4.0279	−44.028	−49.335	2.304 09
9	60	0.16	0.4	−2.7976	−41.798	−44.672	9.682 52
			Mean	−0.3747	−40.573	−45.521	10.6946

Table 6(a) S/N response table for surface roughness (nanofluid with 6% vol. Al_2O_3 nanoparticles)

	Cutting parameter	Mean S/N ratio (dB)				Main effects plot
		Level 1	Level 2	Level 3	Max−Min	
A	Cutting speed	1.0337	−0.4221	−1.7357	2.769 48	
B	Feed rate	2.7009	−1.2386	−2.5864	5.287 33	
C	Depth of cut	0.7163	−0.8008	−1.0395	1.755 91	

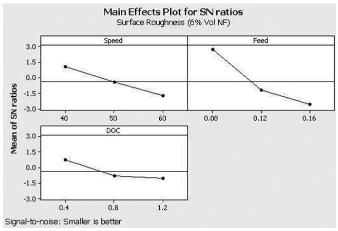

Table 6(b) S/N response table for temperature (nanofluid with 6% vol. Al_2O_3 nanoparticles)

	Cutting parameter	Mean S/N ratio (dB)				Main effects plot
		Level 1	Level 2	Level 3	Max−Min	
A	Cutting speed	−38.296	−41.18	−42.244	3.947 97	
B	Feed rate	−39.069	−39.821	−42.83	3.7606	
C	Depth of cut	−37.44	−40.768	−43.512	6.072 57	

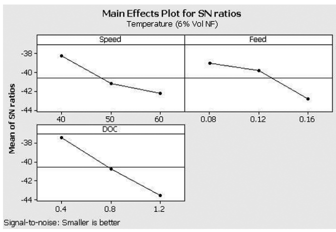

Table 6(c) S/N response table for cutting force (nanofluid with 6% vol. Al_2O_3 nanoparticles)

	Cutting parameter	Mean S/N ratio (dB)				Main effects plot
		Level 1	Level 2	Level 3	Max−Min	
A	Cutting speed	−45.079	−44.724	−46.761	2.0379	
B	Feed rate	−42.833	−47.053	−46.677	4.220 56	
C	Depth of cut	−42.57	−46.845	−47.148	4.578 46	

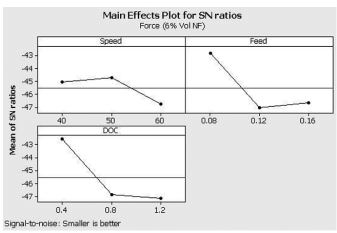

Table 6(d) S/N response table for tool wear (nanofluid with 6% vol. Al_2O_3 nanoparticles)

	Cutting parameter	Mean S/N ratio (dB)				Main effects plot
		Level 1	Level 2	Level 3	Max−Min	
A	Cutting speed	14.789	10.018	7.2765	7.512 86	
B	Feed rate	11.540	15.4071	5.1362	10.2709	
C	Depth of cut	18.602	11.3119	2.169 38	16.4333	

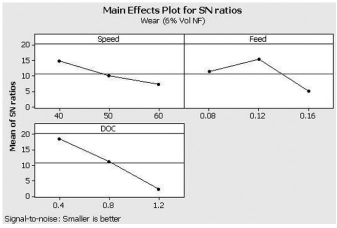

Table 7(a) Optimum conditions for surface roughness

Exp no.	Optimal cutting parameter			Environment	Surface roughness (μm)	
	Speed	Feed	Depth of cut		Predicted value	Experiment value
1	60	0.08	0.4	Dry	0.88	0.91
2	40	0.08	0.4	MQL	0.791	0.823
3	40	0.08	0.4	MQL with NF 4% vol. Al_2O_3	0.663	0.696
4	40	0.08	0.4	MQL with NF 6% vol. Al_2O_3	0.57	0.6

Table 7(b) Optimum conditions for temperature

Exp no.	Optimal cutting parameter			Environment	Surface roughness (μm)	
	Speed	Feed	Depth of cut		Predicted value	Experiment value
1	40	0.08	0.4	Dry	85.480 17	82
2	40	0.08	0.4	MQL	58.8177	56
3	40	0.08	0.4	MQL with NF 4% vol. Al_2O_3	52.382 24	50
4	40	0.08	0.4	MQL with NF 6% vol. Al_2O_3	48.185 97	46

Table 7(c) Optimum conditions for cutting force

Exp no.	Optimal cutting parameter			Environment	Surface roughness (μm)	
	Speed	Feed	Depth of cut		Predicted value	Experiment value
1	50	0.08	0.4	Dry	156.02	148.46
2	50	0.08	0.4	MQL	102.99	98.84
3	50	0.08	0.4	MQL with NF 4% vol. Al_2O_3	93.34	87.67
4	50	0.08	0.4	MQL with NF 6% vol. Al_2O_3	89.99	84.72